Canonical and ETT-mediated auxin signalling pathways synergistically promote gynoecium development in *Arabidopsis thaliana*

Heather M. McLaughlin[1,2], Bhavani Natarajan[1], Lars Østergaard[1]

[1] John Innes Centre, Norwich Research Park, Norwich, NR4 7UH, UK,

[2] The Sainsbury Laboratory, The University of Cambridge, 47 Bateman Street, Cambridge, CB2 1LR, UK

Correspondence

Lars Østergaard (Lars.Ostergaard@jic.ac.uk)

Abstract

Auxin is a phytohormone involved in a wide range of developmental processes. Whilst auxin-mediated signalling is now known to occur through a range of pathways, the transduction of auxin signalling within the carpels has mainly been studied in the context of the ETTIN (ETT) mediated pathway. Several lines of evidence suggest a role for the canonical TIR1/AFB2-mediated pathway in carpel development. However, the relationship between canonical and ETT-mediated mechanisms has not been investigated. Here, *tir1-1 afb2-3 ett-3* triple mutants were generated in *Arabidopsis*, and phenotypic analysis showed synergism between the canonical and ETT-mediated pathways in gynoecium development. Furthermore, ETT shares partial redundancy with ARF4, a close paralog which interacts with the canonical pathway AUX/IAAs. However, the role of ARF4 in the regulation of auxin-responsive gene expression has not been studied in the gynoecium. Here comparative transcriptomics were utilized to assess the roles of ETT and ARF4 in gynoecium development, and the mis-regulation of the auxin response in *ett-3 arf4-2* mutants. The data suggest that the auxin independent mis-regulation of *YABBY2*, *YABBY5,* and *CRABSCLAW* contributes to the abaxial-adaxial identity defects observed in gynoecia and leaves of the double mutant. Auxin sensitive transcriptomics analyses suggest that ETT and ARF4 maintain the auxin insensitivity of both distinct and overlapping targets, many of which become upregulated by auxin in their absence. This is consistent with previously proposed models of A-B ARF antagonism, and suggests that the maintenance of auxin insensitivity at target loci may play an equally important role as the auxin-sensitive induction of genes for a range of developmental processes.

Introduction

The role of auxin in plant development has been widely studied, and auxin signalling is now known to be transduced by several distinct pathways (Dharmasiri et al., 2005; Kepinski & Leyser, 2005; Simonini et al., 2016; Fendrych et al., 2018; Cao et al., 2019; Kuhn et al., 2020; Friml et al., 2022). The canonical auxin signalling pathway induces the expression of auxin sensitive genes in the nucleus (Paponov et al., 2008), and is composed of three main components: Auxin/Indole-3-Acetic Acid repressor proteins (AUX/IAAs), Transport Inhibitor Response1/Arabidopsis F-box (TIR1/AFB) receptors, and Auxin Response Factors (ARFs). In the absence of auxin, ARFs are bound by AUX/IAAs, which recruit the TOPLESS (TPL) co-repressor, preventing the expression of auxin responsive genes (Szemenyei et al., 2008). Auxin acts as a molecular glue that increases the affinity of the TIR1/AFBs for AUX/IAAs. AUX/IAAs are subsequently degraded by the proteasome, allowing ARFs to promote auxin responsive gene expression (Dharmasiri et al., 2005; Kepinski & Leyser, 2005).

ARFs are classified into three distinct clades: A-ARFs, B-ARFs, and C-ARFs (Ulmasov et al., 1999; Tiwari et al., 2003; Finet et al., 2013). A-ARFs are transcriptional activators which readily interact with AUX/IAAs, whilst B and C ARFs are repressive, and interact with AUX/IAAs less readily (Ulmasov et al., 1999; Tiwari et al., 2003; Finet et al., 2013; Vernoux et al., 2011; reviewed in Guilfoyle & Hagen, 2012).

The ETTIN (ETT/ARF3)-mediated pathway was elucidated more recently in the context of its role in gynoecium development (Simonini et al., 2016; Kuhn et al., 2020). ETT is a B-class repressive ARF which lacks the C-terminal domain required for AUX/IAA interaction (Simonini et al., 2016). ETT recruits a TPL-HISTONE DEACETYLASE 19 (HDA19) complex to prevent the transcription of target loci in the absence of auxin. ETT interacts with auxin through its C-terminal ETTIN-SPECIFIC (ES) domain and undergoes a conformational change which breaks the ETT-TPL-HDA19 complex. Histones then become acetylated, and genes can be expressed once more (Kuhn et al., 2020).

ett mutants exhibit severe gynoecium defects which phenocopy aberrations produced upon treatment with the auxin transport inhibitor N-1-Naphthylphthalamic Acid (NPA), highlighting the importance of ETT-mediated signalling for auxin related processes in carpel development (Nemhauser et al., 2000). Gynoecium morphogenesis is dependent on the dynamic distribution of auxin (Moubayidin and Østergaard, 2014). However, studies on auxin signal transduction in the carpels have mainly focused on the role of the ETT-mediated pathway (Simonini et al., 2016; Simonini et al., 2017; Kuhn et al., 2020). An understanding of the relative contribution of canonical and ETT-mediated signalling to gynoecium development remains lacking, although several lines of evidence implicate the canonical pathway in this process.

Four of the canonical auxin receptors - *TIR1*, *AFB1*, *AFB2*, and *AFB3* - are expressed in the style of the developing *Arabidopsis* gynoecium (Dharmasiri et al., 2005; Cecchetti et al., 2008).

Higher order *tir1afb1245* mutants exhibit curled siliques and reduced fertility indicative of gynoecium defects, and infrequently produce siliques with only one valve (Prigge et al., 2020). AUX/IAA interacting ARFs, which are therefore implicated in canonical auxin signalling (Vernoux et al., 2011; Piya et al., 2014), are also involved in the regulation of gynoecium development (Nagpal et al., 2005; Wang et al., 2005; Pekker et al., 2005; Kelley et al., 2012), further supporting a role for the canonical pathway.

ETT shares partial redundancy with its paralogous ARF, ARF4, which contains a C-terminal PB1-domain and is capable of AUX/IAA interaction (Pekker et al., 2005; Kelley et al., 2012; Finet et al., 2010; Vernoux et al., 2011). However, whilst the transcriptional targets of ETT are well described (Simonini et al., 2017; Andres-Robin et al., 2020), those of ARF4 are not.

Here, *tir1-1 afb2-3 ett*-3 mutants were generated in *Arabidopsis.* The triple mutant showed exacerbation of the *ett-3* phenotype suggesting that the canonical and ETT-mediated pathways function synergistically in gynoecium development. As little is known about the global transcriptional regulation of genes by ARF4, a comparative transcriptomics analysis was conducted to elucidate how ETT and ARF4 regulate targets, and to what extent these targets overlap. The data presented suggest that the regulation of gynoecium development by ETT and ARF4 is two-fold. Firstly, ETT and ARF4 redundantly regulate targets involved in cell fate specification independently of auxin, and the mis-regulation of these genes correlates with phenotypes observed in the double mutant. Secondly, ETT and ARF4 redundantly maintain auxin insensitivity at target loci involved in the regulation of pectin, the mis-regulation of which has previously been linked to morphogenesis defects within the *ett* gynoecium (Andres-Robin et al., 2018). Most redundantly regulated targets became downregulated in response to auxin in the *ett-3 arf4-2* mutant, whilst a subset of targets became upregulated. ETT and ARF4 maintain the auxin insensitivity of a range of targets, which became upregulated in response to auxin upon their mutation, suggesting that A-B ARF antagonism previously observed in *Marchantia* (Kato et al., 2020) and *Physcomitrium* (Lavy et al., 2016) may also regulate gene expression in *Arabidopsis.* Together, the findings presented reveal crosstalk between the canonical and ETT-mediated pathway and suggest that the maintenance of auxin insensitivity at target loci plays an important role in a range of processes.

Results

Phenotypic analyses suggest synergism between canonical and ETT-mediated pathways

To understand the relationship between the canonical and ETT-mediated auxin signalling pathways during gynoecium development, *tir1-1 afb2-3 ett-3* triple mutants were generated in *Arabidopsis*, and the resulting phenotypes were assessed (Figure 1, Supplemental Figure 1).

111 The *ett-3* mutant exhibited reduced valves, a loss of radialization in the style, and over-
112 proliferation of stigmatic tissues at later developmental stages, whilst the *arf4-2* and *tir1-2*
113 *afb2-3* mutants resembled Col-0 (Figure 1, Supplemental Figure 1). The *ett-3* phenotype was
114 exacerbated in both *ett-3 arf4-2* and *tir1-1 afb2-3 ett-3*. Valves in *ett-3 arf4-2* gynoecia were
115 significantly reduced, producing an open ovary with ectopic ovules and few stigmatic papillae
116 (Figure 1, Supplemental Figure 1). The *ett-3 arf4-2* gynoecia lacked a style and split into two
117 distinct lobes with stigmatic papillae at their tips. Similarly, *tir1-1 afb2-3 ett-3* mutants exhibited
118 enhanced valve reduction relative to *ett-3* mutants, producing a partially open ovary with
119 ectopic ovules, and no discernable style or replum (Figure 1, Supplemental Figure 1). The
120 stigmatic papillae in *tir1-1 afb2-3 ett-3* gynoecia also developed atop two lobes produced at
121 the apex, and exhibited over proliferation of stigmatic tissues at later developmental stages
122 comparable to those observed in *ett-3* (Figure 1, Supplemental Figure 1).
123 The exacerbation of the *ett-3* phenotype by *tir1-1 afb2-3* mutation demonstrates that the
124 canonical and ETT-mediated pathways function synergistically to promote gynoecium
125 development. Furthermore, the phenotypic similarities between *ett-3 arf4-2* and *tir1-1 afb2-3*
126 *ett-3* mutants, especially at the early stages of gynoecium development, suggest that
127 ETT/ARF4 and TIR1/AFB2 regulate similar processes in gynoecium development.
128
129 **Comparative transcriptomics analysis of auxin independent and auxin sensitive**
130 **ETT/ARF4 targets**
131 ETT is known to function partially redundantly with ARF4 in the regulation of gynoecium
132 development (Pekker et al., 2005; Finet et al., 2010; Kelley et al., 2012). Whilst ETT-mediated
133 signalling and the regulation of ETT-target genes are relatively well studied (Simonini et al.,
134 2016; Simonini et al., 2017; Kuhn et al., 2020), a global understanding of how ARF4 regulates
135 its targets, and which genes it modulates in conjunction with ETT, is lacking. ARF4 is known
136 to physically interact with AUX/IAAs (Vernoux et al., 2011), implicating it in the canonical
137 pathway.
138 To better understand how ARF4 regulates its targets both alone and together with ETT, a
139 comparative transcriptomic analysis (RNA sequencing, from here on RNA-Seq) was
140 conducted utilizing whole inflorescence tissues of Col-0, *ett-3, arf4-2, and ett-3 arf4-2* lines
141 treated with 100 μM Indole-3-Acetic Acid (IAA) and 10 μM N-1-Naphthylphthalamic Acid (NPA)
142 or mock treatments for one hour.
143 A principal component analysis revealed that the lines differed more by genotype than by
144 auxin treatment (Supplemental Figure 2), and many genes which are reportedly auxin
145 responsive (Paponov et al., 2008) were modulated in response to auxin in wildtype plants,
146 indicating that the auxin treatment was effective (Supplemental Table 1). *PINOID*, a previously
147 well-characterized ETT target (Simonini et al., 2016; Simonini et al., 2017; Kuhn et al., 2019)

148 which is upregulated in wildtype in response to auxin (Kuhn et al., 2020) was not identified as
149 an auxin sensitive gene within this study. Previous transcriptomics analyses aiming to identify
150 ETT targets utilized different schedules of auxin treatment (Kuhn et al., 2020; Simonini et al.,
151 2017) which may explain the observed discrepancies. Significant overlap was however
152 observed between genes mis-regulated in *ett-3* mutants between this study and Simonini et
153 al., 2017 (Supplemental Figure 3, Supplemental Table 2 and 3).
154 Two analyses were conducted on the resulting RNA-Seq data: an auxin independent analysis
155 which aimed to assess the developmental roles of ETT and ARF4 independently of auxin, and
156 an auxin sensitive analysis which assessed how the auxin responses vary from wildtype in the
157 mutants.
158
159 **ETT and ARF4 are implicated in the regulation of cell fate commitment independently**
160 **of auxin**
161 The auxin independent analysis was conducted in accordance with the schema in
162 Supplemental Figure 4. Two datasets each consisting of three lists of genes were used for
163 this analysis. The first dataset comprised lists of genes which were differentially expressed
164 relative to wildtype in *ett-3*, *arf4-2,* and *ett-3 arf4-2* after mock treatment, whilst the second
165 dataset comprised the same after IAA treatment. These lists were compared in Venny 2.1 to
166 generate two three-way Venn diagrams, one for each dataset. The data were then compared
167 across mock and auxin treatments to identify genes which are mis-regulated in the same
168 manner in both datasets. Any auxin sensitive genes within these lists were removed, leaving
169 genes which are regulated by ETT and ARF4 independently of auxin. Based on where these
170 genes positioned within a three-way Venn diagram, models of gene behavior were devised
171 which may explain the observed patterns of statistical significance (Figure 2 A and B).
172
173 Heatmaps were generated to assess whether genes followed the proposed models of
174 regulation, and Gene Ontology (GO) term analyses using PANTHER statistical
175 under/overrepresentation tests were conducted to identify biological processes which are
176 enriched within each target category (Figure 3).
177 The transcriptomics analysis identified 98 genes (53 up, 45 down) which were significantly
178 mis-regulated in *ett-3 arf4-2* relative to wildtype in accordance with their redundant regulation
179 by ETT and ARF4 (Figure 2B and C, Supplemental Figure 5). GO term analysis indicated
180 significant enrichment within this list for genes involved in cell fate commitment (Figure 3),
181 including *CLAVATA3/ESR-RELATED 19* (*CLE19*), *NO TRANSMITTING TRACT* (*NTT*), and
182 *FAMA*, which were significantly upregulated; and *YABBY2* (*YAB2*) and *YAB5* which were
183 significantly downregulated in *ett-3 arf4-2* (Figure 4). The mis-regulation of *YABBY* genes in

184 *ett-3 arf4-2* is consistent with the abaxial-adaxial axis defects present within the leaves and
185 gynoecia of this line (Figure 1, Supplemental Figure 6).
186 Whilst *FAMA* was upregulated in *ett-3 arf4-2*, *TOO MANY MOUTHS* (*TMM*), another regulator
187 of the stomatal lineage, was constitutively downregulated (Supplemental Figure 5). Along with
188 the mis-regulation of stomatal lineage genes in *ett-3 arf4-2*, stomatal defects, such as stomatal
189 clustering on laminal outgrowths on the abaxial leaf surface, were also observed
190 (Supplemental Figure 6). The constitutive upregulation of the WUSCHEL related homeobox
191 transcription factor *WOX9*, and the CLV3 related peptide encoding gene *CLE19* (Figure 4,
192 Supplemental Figure 5), were observed in *ett-3 arf4-2*, along with variability in the numbers of
193 floral organs produced within flowers (Supplemental Figure 6). Finally, the auxin biosynthesis
194 gene *TAA1*, which promotes the production of auxin through the IPA pathway, was
195 constitutively upregulated in the double mutant (Supplemental Figure 5), suggesting that auxin
196 biosynthesis is also regulated redundantly by ETT and ARF4 independently of auxin.
197 Together, these data correlate with phenotypes observed in the *ett-3 arf4-2* mutant and
198 suggest that ETT and ARF4 may redundantly regulate cell fate specification independently of
199 auxin in a range of biological contexts, including the abaxial-adaxial axis of lateral organs and
200 the stomatal cell lineage.
201 Targets which became similarly mis-regulated in all mutant backgrounds, consistent with their
202 regulation by ETT-ARF4 heterodimers (151 genes, 56 up, 95 down; Supplemental Figure 7)
203 showed significant enrichment for involvement in gluco- and glycosinolate related secondary
204 metabolic processes (Figure 2, A, B and C; Figure 3). However, glucosinolate-related
205 phenotypes were not assessed within this study. These data suggest a role for ETT and ARF4
206 in the regulation of metabolic processes independently of auxin, and suggest that ETT and
207 ARF4 may regulate genes as heterodimers. Consistent with this hypothesis, interactions were
208 observed between ETT and ARF4 in yeast two hybrid assays. This interaction required the N-
209 terminal DNA Binding domain of ARF4, and was insensitive to auxin (Supplemental Figure 8).
210 The 76 targets which became similarly mis-regulated in both *ett-3* and *ett-3 arf4-2*, consistent
211 with their ETT-specific regulation, included *INDEHISCENT* (*IND*), *JAGGED* (*JAG*), and
212 *CRABSCLAW* (*CRC*), which have previously been implicated in gynoecium development
213 (Figure 5).
214 Whilst the *arf4-2* mutant appeared as wildtype (Figure 1), 49 ARF4-specific genes were
215 identified (Supplemental Figure 9). This list was not enriched for any specific biological
216 processes and did not contain any known regulators of gynoecium development, suggesting
217 that ARF4 mainly functions in conjunction with ETT to elicit its auxin-independent effects in
218 the carpels.
219 Together, these data suggest that ETT and ARF4 regulate distinct and overlapping targets
220 independently of auxin to promote gynoecium development.

221

222 **Analysis of auxin sensitivity in ETT/ARF4 targets**

223 Gynoecium morphogenesis is dependent on the dynamic distribution of auxin (Moubayidin &
224 Østergaard, 2014), and gynoecium defects of *ett-3 arf4-2* mutants suggest a role for ETT and
225 ARF4 in the transduction of auxin signalling (Pekker et al., 2005). A second analysis was
226 therefore conducted to assess how the auxin response varies from wildtype in the mutants.
227 Genes which were significantly auxin responsive in wildtype were compared to genes which
228 were significantly auxin responsive in each mutant background (*ett-3*, *arf4-2,* and *ett-3 arf4-*
229 *2*). Models of gene behaviour were devised, which may explain the patterns of statistical
230 significance observed for genes that fall into specific segments of a 4-way Venn diagram
231 (Figure 6). Evidence was found in the experimental data to support the following models of
232 gene regulation: genes are redundantly regulated by ETT and ARF4 to prevent their auxin
233 responsiveness (Figure 6B3); genes are regulated by ETT-ARF4 heterodimers which promote
234 (Figure 6B4) and prevent (Figure 6B10) their auxin responsiveness; the auxin insensitivity of
235 genes is specifically promoted by ARF4 (Figure 6B6); and genes are regulated by auxin
236 independently of ETT and ARF4 (Figure 6B8).

237

238 **ETT and ARF4 redundantly prevent the auxin sensitivity of target genes**

239 The auxin sensitive analysis identified 179 genes which were auxin sensitive only in the *ett-3*
240 *arf4-2* mutant background (44 up and 135 down upon auxin treatment; Figure 6A, B3, C,
241 Figure 7). This suggests that these genes are redundantly regulated by ETT and ARF4 to
242 maintain their auxin insensitivity. PANTHER statistical over/under-representation analysis
243 showed that this list was enriched for genes involved in the regulation of pH, pectin catabolism,
244 and cell wall organization (Supplemental Figure 10). As the regulation of cell wall organization
245 has previously been linked to auxin-mediated cell expansion (Majda and Robert, 2018) and
246 organogenesis (Traas, 2019), the expression profiles of these genes were analysed in more
247 detail (Figure 8). Targets implicated in pectin metabolism and cell wall organization included
248 the *PECTIN METHYLESTERASES* (*PMEs*) *PME23*, *PME28*, *PME48*, *PME49*, *PPME1,* and
249 *VGDH2 (VANGUARD 1 HOMOLOG 2)*; and six members of the pectin lyase superfamily
250 *AT1G05660*, *AT3G07850*, *AT5G48140*, *AT3G07830*, *AT3G07840*, *AT3G14040* (Figure 8). In
251 all cases, these genes became significantly downregulated in response to auxin only in the
252 *ett-3 arf4-2* background, suggesting that ETT and ARF4 redundantly promote their expression
253 in the presence of auxin to prevent their downregulation (Figure 8).

254

255

256 **ETT/ARF4 targets conform to models of auxin sensitive heterodimer regulation**

257 Genes were identified within the auxin sensitive analysis which conformed to the heterodimer-
258 mediated model of regulation (Figure 6, A, B4 and B10, C). 46 genes (36 up and 10
259 downregulated upon auxin treatment) were auxin sensitive in wildtype, and auxin insensitive
260 in all mutant backgrounds, consistent with a model in which ETT-ARF4 heterodimers promote
261 their auxin sensitivity (Figure 6 A, B4, C, Supplemental Figure 11). This list was significantly
262 enriched for genes involved in the regulation of secondary metabolic processes relating
263 glucosinolates (Supplemental Figure 12). A further 143 genes were auxin insensitive in
264 wildtype and upregulated in response to auxin in all mutant backgrounds, suggesting that ETT-
265 ARF4 dimers maintain auxin insensitivity at these loci (Figure 6, A, B10, C Supplemental
266 Figure 13). The upregulation of these genes in response to auxin in all mutant backgrounds is
267 consistent with A-B ARF antagonism previously observed in *Marchantia polymorpha* and
268 *Physcomitirium patens* (Kato et al., 2020; Lavy et al., 2016). Consistent with this hypothesis,
269 *ARF5*, *ARF6,* and *ARF8*, which are A-class activators, are expressed in the gynoecium along
270 with ETT and ARF4 at various stages of development (Supplemental Figure 14). The list of
271 targets whose auxin insensitivity is maintained by ETT-ARF4 dimers was enriched for targets
272 involved in the negative regulation of defence responses (Supplemental Figure 12). No known
273 regulators of gynoecium development were found within the lists of genes which conformed
274 to heterodimer mediated regulation, suggesting that this mode of gene activity does not
275 directly regulate auxin-mediated carpel development, but may be involved in the regulation of
276 other biological processes.

277 **ARF4 prevents the auxin sensitivity of specific targets independently of ETT**

278 199 genes were identified which were similarly mis-regulated in *arf4-2* and *ett-3 arf4-2* mutants
279 (five down, 194 upregulated upon auxin treatment; Figure 6A, B6, C, Figure 9), consistent with
280 their ARF4-specific regulation. These genes were auxin insensitive in wildtype and became
281 auxin sensitive in both mutant lines, implying that ARF4 maintains their auxin insensitivity. The
282 upregulation of these targets in response to auxin in *arf4-2* and *ett-3 arf4-2* is consistent with
283 previously proposed models of A-B ARF antagonism (Kato et al., 2020; Lavy et al., 2016). The
284 list of ARF4 specific targets is significantly enriched for genes involved in the regulation of fruit
285 ripening and processes relating to ethylene biosynthesis (Supplemental Figure 15).
286
287
288
289

290
291 ## Discussion
292
293 **Synergism between canonical and ETT-mediated signalling**
294 Prior to this study, several lines of evidence implicated the canonical pathway in the regulation
295 of gynoecium development, including carpel defects observed in higher order *tir1/afb* mutants
296 and class A-ARF mutants (Prigge et al., 2020; Nagpal et al., 2005); and the expression of
297 canonical pathway receptor genes in the gynoecium (Cechetti et al., 2008; Dharmasiri et al.,
298 2005). However, the relationship between the canonical and ETT-mediated pathways had not
299 been dissected. The data presented here indicate synergism between the canonical and ETT-
300 mediated pathway and suggest that ETT functions with ARF4 to regulate both distinct and
301 overlapping targets.
302 ARF4 has previously been shown to interact with AUX/IAA proteins (Vernoux et al., 2011; Piya
303 et al., 2014), implicating ARF4 in the canonical pathway. However, whether such interactions
304 have a biological relevance *in planta* remains unknown. In *Marchantia*, the overexpression of
305 repressive ARFs suppresses the constitutive auxin response phenotypes observed in *aux/iaa*
306 mutants (Lavy et al., 2016), suggesting that repressive ARFs can transcriptionally regulate
307 genes without AUX/IAA interactors. Whilst this is certainly true for *Arabidopsis* ETT, which
308 lacks the C-terminal domain required for AUX/IAA interaction, the C-terminal AUX/IAA
309 interacting domain of ARF4 is necessary for ARF4 functionality in the gynoecium (Finet et al.,
310 2010).
311 In the canonical model of auxin signalling, AUX/IAAs allow the recruitment of TOPLESS
312 related co-repressors to loci to switch off their expression in the absence of auxin (Causier et
313 al., 2012). However, ETT and ARF4 contain repressor motifs which facilitate direct co-
314 repressor recruitment (Lokerse and Weijers, 2009). The auxin sensitive interaction between
315 ETT and TPL underpins the repression of genes in the absence of auxin in the ETT-mediated
316 pathway (Kuhn et al., 2020). Future work will be required to unpick the relevance of ARF4-
317 AUX/IAA and direct ARF4-TPL interactions to gain a better understanding of the mechanisms
318 regulating ARF4 activity.
319
320
321 **Comparative transcriptomics correlate with phenotypic defects observed in *ett-3 arf4-***
322 ***2* mutants**
323 The auxin sensitive analysis identified distinct and overlapping targets of ETT and ARF4.
324 Targets under the auxin-independent redundant regulation of ETT and ARF4 included the
325 YABBY TFs *YAB2* and *YAB5*, whilst *CRC* was mis-regulated in both *ett-3* and *ett-3 arf4*-2,
326 consistent with its ETT-specific regulation. YABBY proteins specify abaxial identity along with

327 the KANADI family of transcription factors (Eshed et al., 2004). ETT and ARF4 function co-
328 operatively with KANADI proteins to promote abaxial cell fate of lateral organs (Pekker et al.,
329 2005). Laminal outgrowths from the abaxial leaf surface have previously been observed in
330 *kan1 kan2* loss of function mutants. This phenotype is suppressed in *yab1 yab3 yab5* (Eshed
331 et al., 2004) and *yuc1 yuc2 yuc4* backgrounds (Wang et al., 2011), suggesting that the
332 production of outgrowths is dependent on YABBYs and auxin biosynthesis. Similar outgrowths
333 were observed on the abaxial surface of *ett-3 arf4-2* mutant leaves in this study, consistent
334 with previously proposed roles for ETT/ARF4 in KANADI-mediated signalling (Pekker et al.,
335 2005). However, given that *YAB2*, *YAB5,* and *CRC* were significantly downregulated in the
336 *ett-3 arf4-2* mutant background, it is unclear if these outgrowths are YABBY dependent. Whilst
337 *yabby* single mutants lack obvious abaxial-adaxial identity defects, higher order mutants show
338 significant alterations in abaxial-adaxial polarity (Sarojam et al., 2010; Siegfried et al., 1999).
339 The downregulation of multiple *YAB* transcription factors within the *ett-3 arf4-2* mutant is
340 therefore consistent with the abaxial-adaxial identity defects observed in the leaves and
341 gynoecia of the double mutant in this study.
342 Previous studies reported reduced valve margin definition in *ind* (Liljegren et al., 2004), and
343 apical gynoecium defects in *jag* and *crc* mutants (Bowman & Smyth, 1999; Ohno et al., 2004).
344 Similar gynoecium defects were exhibited in this study by *ett-3* and *ett-3 arf4-2* (Figure 1),
345 along with the constitutive downregulation of *IND, JAG,* and *CRC,* which is consistent with the
346 previously proposed roles of these genes in gynoecium development. Future studies should
347 aim to determine which of the targets identified within this study are direct/indirect ETT/ARF4
348 targets.
349
350
351
352 **Auxin Sensitive analysis suggests ETT and ARF4 maintain auxin insensitivity at target**
353 **loci**
354 Previous studies in *Marchantia polymorpha* and *Phiscomitrium patens* found antagonism
355 between A- and B-ARFs to regulate the auxin sensitivity of tissues (Kato et al., 2020; Lavy et
356 al., 2016), with the auxin response being promoted by A-ARFs and inhibited by B-ARFs.
357 Consistent with this model of B-ARF function, ETT and ARF4 were previously shown to
358 repress auxin responses in an *Arabidopsis* root hair system (Choi et al., 2018). The
359 transcriptomics data presented here suggest that ETT and ARF4 largely prevent the auxin
360 sensitivity of distinct and overlapping targets, many of which become upregulated in response
361 to auxin in various mutant backgrounds, consistent with models of A/B-ARF antagonism.
362 However, many of their redundantly regulated targets, including genes involved in pectin
363 methylesterification, pectin catabolism, and cell wall organisation become downregulated in

364 response to auxin. Auxin-mediated repression has been observed in TMK-mediated
365 signalling, where atypical AUX/IAAs are stabilized in the presence of auxin (Cao et al., 2019).
366 However, it is unclear if such a mechanism functions in the gynoecium. Previous studies have
367 implicated PME family members in the regulation of cell wall stiffness during gynoecium
368 development in *ett* mutants and showed that ETT promotes PME expression in the carpels
369 (Andres-Robin et al., 2018; Andres-Robin et al., 2020). Furthermore, the overexpression of
370 *PECTIN METHYLESTERASE INHIBITOR 3* (*PMEI3*), which antagonises PME activity,
371 phenocopied the valve reductions observed in *ett* mutants (Andres-Robin et al., 2018). Taken
372 together with these previous studies, the data presented here suggest that ETT and ARF4
373 may redundantly promote the expression of *PMEs* to prevent their downregulation in response
374 to auxin, and the mis-regulation of these genes may contribute to the gynoecium defects
375 observed in *ett-3 arf4-2*.
376 The data presented suggest that ETT functions alongside ARF4 to prevent the expression of
377 genes which would otherwise become auxin sensitive in its absence, possibly through the
378 activity of A-ARFs with which they are co-expressed, or due to the activity of TMK-related
379 pathways in the case of auxin-downregulated genes. The data also suggest that the
380 maintenance of genes in an auxin insensitive state may be equally as important as the
381 promotion of auxin sensitivity at other loci to facilitate normal growth and development. Future
382 studies should continue to dissect the relationships between distinct auxin signalling pathways
383 to gain a greater understanding of the wider auxin signalling network, allowing for a more
384 global perspective of auxin-mediated plant development.
385

386 ## Materials and Methods

387 ### Plant materials and growth conditions

388 Seeds were sown onto damp soil (Levington F2 compost with Intercept and grit at a 6:1 ratio)
389 and stratified for 3 days at 4°C in the dark before transferal to a controlled environment room
390 (CER) and growth in long day conditions (16 hours light/8 hours dark, 22°C). All mutant lines
391 were generated in a Col-0 background.

392 Mutant and transgenic lines used in this work which have been previously published are: *ett-*
393 *3* (Sessions et al., 1997; Simonini et al., 2016), *arf4-2* (SALK_070506, Alonso et al., 2003)
394 and *tir1-1 afb2*-3 (Parry et al., 2009). The *ett-3 arf4-2* line was generated by crossing the *ett-*
395 *3* line and *arf4-2* (SALK_070506). The *tir1-1 afb2-3 ett-3* line was generated by crossing *ett-*
396 *3* with *tir1-1 afb2-3*. The PCR conditions and genotyping primers used for these lines are
397 listed in Supplemental Table 4 and Supplemental Table 5. Additional information relating to

398 the genotyping of each line can also be found in the supplemental material and methods.
399 *pARF3/ETT: GFP*, *pARF4: GFP*, *pARF5: GFP*, *pARF6: GFP* and *pARF8: GFP* are
400 previously published (Rademacher *et al*., 2011).

401

402 **Scanning Electron Microscopy**

403 Whole inflorescences were harvested and incubated in fixative (3.7% formaldehyde, 3% acetic
404 acid and 50% ethanol) for 16 hours at room temperature on a shaker. The fixative was
405 aspirated, and the tissues were washed in an ethanol series (70%, 80%, 90% and 100%) at
406 room temperature on a shaker. Each wash was incubated for 30 minutes. The samples were
407 then washed twice for 30 minutes in 100% dry ethanol and critical point dried with carbon
408 dioxide using a Leica CPD300. Gynoecia were dissected onto stubs and gold coated using an
409 Agar high resolution sputter coater. Imaging was conducted with a Zeiss Supra 55VP Field
410 Emission Scanning Electron Microscope using a 3kV acceleration voltage.

411 **RNA sequencing Analysis**

412 Whole inflorescences were harvested from Col-0, *ett-3*, *arf4-2,* and *ett-3 arf4-2* lines treated
413 with either mock (dH2O, 0.1% tween, 0.1% ethanol) or 100 µM IAA and 10µM NPA (dissolved
414 in ethanol), 0.1% tween for one hour. Three biological replicates were harvested for each
415 genotype one hour after treatment. Each replicate contained pooled material from three plants.
416 The tissue was snap frozen in liquid nitrogen and RNA extraction was conducted using a
417 Qiagen RNeasy Plant Mini Kit with on-column DNase treatment, in accordance with the
418 manufacturer's guidelines. The RNA quality was assessed by gel electrophoresis, and the
419 RNA concentration was measured using a nanodrop (ThermoFisher), and the RNA integrity
420 was tested using a Bioanalyzer 2100 (Agilent). Novogene (Hong Kong), conducted cDNA
421 library preparation (250-300 bp insert cDNA library), and sequencing (20M pair reads), the
422 details of which can be found in the supplemental materials and methods.

423 **Principle Component Analysis**

424 Principle component analysis was conducted in iDEP 9.1 (http://ge- lab.org/idep/, (Ge et al.,
425 2018)) on expression values normalised to fragments per kilobase of transcript per million
426 mapped reads (FPKM).

427

428

429 **Analysis of auxin independent ETT/ARF4 targets**

430 This analysis was conducted using the differentially expressed gene lists provided by
431 Novogene (Hong Kong). Six lists of differentially expressed genes were used in this analysis:
432 (1) *arf4-2* vs Col-0 mock; (2) *ett-3* vs Col-0 mock; (3) *ett-3 arf4-2* vs Col-0 mock; (4) *arf4-2* vs
433 Col-0 IAA; (5) *ett-3* vs Col-0 IAA; and (6) *ett- 3 arf4-2* vs Col-0 IAA. Only genes which were at
434 least 2-fold up or downregulated in at least one background were included in this analysis
435 (log2fold value of >1 or < -1). Analyses were conducted with Venny (Version 2.1;
436 https://bioinfogp.cnb.csic.es/tools/venny/index.html; Oliveros, 2007) to identify genes mis-
437 regulated only in one background, mis-regulated only in two backgrounds, or mis-regulated in
438 all three backgrounds relative to wildtype. The mock and auxin treated datasets were
439 independently assessed using Venny, and then compared to identify genes which were
440 similarly differentially expressed in both the presence and absence of auxin. Finally, any genes
441 which were significantly differentially expressed (2-fold up or down-regulated in at least one
442 background) in response to auxin were removed from the lists, leaving only those genes which
443 were regulated independently of auxin.

444 **Analysis of auxin sensitive ETT/ARF4 targets**

445 The auxin sensitive analysis utilized DEGs from the following lists generated by Novogene
446 (Hong Kong): (1) Col-0 IAA vs Col-0 mock; (2) *ett-3* IAA vs *ett-3* mock; (3) *arf4-2* IAA vs *arf4-*
447 *2* mock; and (4) *ett-3 arf4-2* IAA vs *ett-3 arf4-2* mock. The genes which were differentially
448 expressed in each background in response to auxin were then compared to reveal how the
449 auxin response in each mutant differed from WT. Venny (Version 2.1) was utilized to generate
450 a four-way Venn diagram.

451 **Heatmap Analysis**

452 Heatmapper (Babicki et al., 2016) was utilized to generate heatmaps showing the average
453 FPKM for genes in each category in both the auxin independent and auxin sensitive
454 analyses. The settings used in Heatmapper were as follows: Scale type was set to row;
455 colour brightness to 50; number of shades = 50; colour scheme red/green; clustering method
456 average linkage; distance measurement method Spearman rank correlation; clustering
457 applied to rows; and dendrograms were shown for rows.

458

459

460 **Go Term Analysis**

461 Gene Ontology (GO) term analysis was conducted on the lists of genes which fell into each
462 category of the Venn diagrams in both the auxin independent and auxin sensitive analyses to
463 identify whether these lists were enriched for genes involved in specific biological processes.
464 This GO term analysis was conducted using a statistical under/over-representation test, which
465 utilizes Fisher's Exact Test for p value estimation ($p<0.05$). The GO term analysis utilized the
466 PANTHER classification system (Mi et al., 2019).

467

468 **Yeast 2 Hybrid**

469 The full-length coding sequence of *ETT* and *ARF4* and truncated *ARF4* fragments were
470 amplified by PCR using primers designed for gateway cloning (Supplemental Table 6). The
471 resulting PCR products were purified using a Qiagen QIAquick PCR purification kit and
472 introduced in the gateway entry vector pDONR207 (Life Technologies) by BP clonase
473 reactions, in accordance with the Thermo-Fisher Gateway protocol. The products of this
474 reaction were transformed into DH5α cells (Invitrogen) according to the manufacturer's
475 guidelines and grown on LB agar plates containing gentamycin (10 µg/ml) overnight at 37 $^{\circ}$C.
476 Constructs were validated by colony PCR and sequencing. The ARF sequences within
477 pDONR207 were then recombined into the pGAD-T7 and pGBK-T7 (Clontech) expression
478 vectors by LR clonase reactions, transformed into *E. coli*, and once more validated by colony
479 PCR and sequencing. The expression vectors were then co-transformed into AH109
480 *Saccharomyces cerevisiae* (Clontech), by lithium acetate mediated transformation (Gietz and
481 Schiestl, 2007). Different combinations of AD (pGAD-T7) and BD (pGBK-T7) vectors, or empty
482 vector controls, were introduced in pairs to competent yeast cells to determine whether ARF4
483 and ETT interact, and through which domains of ARF4. Transformants were plated onto YSD
484 -W-L media and grown at 28°C for 72 hours, before serial dilution (10^0, 10^1, 10^2, and 10^3) and
485 plated onto YSD -W-L-H-A plates to assess interactions. After plating on selective media,
486 yeast colonies were photographed after growth at 28°C for 7 days. Figures were created using
487 images from the 10^1 dilution in all cases. Auxin sensitivity was assessed by adding 100 µM
488 IAA (Sigma) to the medium.
489
490

Confocal Microscopy

Stage 8-14 gynoecia were dissected from the plant and placed onto slides in water containing 0.015% Silwet L-77 (De Sangosse Ltd.) to prevent the formation of bubbles. Cover slips were then applied, and the gynoecia were imaged using a Leica SP5 confocal microscope (HyD detector, Smart Gain 30% 200hz, 4x Line Average) with a 40x water immersion lens. GFP was excited at a wavelength of 488 nm and detected at 498–530 nm. Images were taken as Z-stacks, and then processed in Image J 1.48 to form composite 3D projections, which were then converted to RGB images.

Author contribution

H.M.M. and L.Ø. devised the experiments. H.M.M. and B.N. conducted experiments. H.M.M. wrote the manuscript.

Acknowledgements

Apologies to any colleagues whose work we have not cited due to space limitations. Special thanks to Yang Dong (IBCAS) for his continued input and collaboration on this project; to Henrik Jönsson (SLCU) for supporting the completion of the project; and to James McLaughlin (EMBL-EBI) for bioinformatics support. H.M.M. was funded by the John Innes Foundation (at JIC) and the Gatsby Charitable Foundation (at SLCU, GAT3395-PR4B), B.N. by BBSRC (BB/S002901/1) and L.Ø. by BBSRC (BB/P013511/1).

524 **References**

525 Alonso JM, Stepanova AN, Leisse TJ, Kim CJ, Chen H, Shinn P, Stevenson DK, Zimmerman
526 J, Barajas P, Cheuk R, Gadrinab C, Heller C, Jeske A, Koesema E, Meyers CC, Parker
527 H, Prednis L, Ansari Y, Choy N, Deen H, Geralt M, Hazari N, Hom E, Karnes M,
528 Mulholland C, Ndubaku R, Schmidt I, Guzman P, Aguilar-Henonin L, Schmid M, Weigel
529 D, Carter DE, Marchand T, Risseeuw E, Brogden D, Zeko A, Crosby WL, Berry CC, Ecker
530 JR. 2003. Genome-wide insertional mutagenesis of Arabidopsis thaliana. *Science (1979)*
531 **301**. doi:10.1126/science.1086391

532 Andres-Robin A, Reymond MC, Brunoud G, Martin-Magniette ML, Monéger F, Scutt CP. 2020.
533 Immediate targets of ETTIN suggest a key role for pectin methylesterase inhibitors in the
534 control of Arabidopsis gynecium development. *Plant Signal Behav* **15**.
535 doi:10.1080/15592324.2020.1771937

536 Andres-Robin A, Reymond MC, Dupire A, Battu V, Dubrulle N, Mouille G, Lefebvre V, Pelloux
537 J, Boudaoud A, Traas J, Scutt CP, Monéger F. 2018. Evidence for the regulation of
538 gynoecium morphogenesis by ETTIN via cell wall dynamics. *Plant Physiol* **178**.
539 doi:10.1104/pp.18.00745

540 Babicki S, Arndt D, Marcu A, Liang Y, Grant JR, Maciejewski A, Wishart DS. 2016.
541 Heatmapper: web-enabled heat mapping for all. *Nucleic Acids Res* **44**.
542 doi:10.1093/NAR/GKW419

543 Cao M, Chen R, Li P, Yu Y, Zheng R, Ge D, Zheng W, Wang X, Gu Y, Gelová Z, Friml J,
544 Zhang H, Liu R, He J, Xu T. 2019. TMK1-mediated auxin signalling regulates differential
545 growth of the apical hook. *Nature* **568**. doi:10.1038/s41586-019-1069-7

546 Cecchetti V, Altamura MM, Falasca G, Costantino P, Cardarelli M. 2008. Auxin regulates
547 Arabidopsis anther dehiscence, pollen maturation, and filament elongation. *Plant Cell*
548 **20**:1760–1774. doi:10.1105/tpc.107.057570

549 Choi HS, Seo M, Cho HT. 2018. Two TPL-binding motifs of ARF2 are involved in repression
550 of auxin responses. *Front Plant Sci* **9**. doi:10.3389/fpls.2018.00372

551 Dharmasiri N, Dharmasiri S, Weijers D, Lechner E, Yamada M, Hobbie L, Ehrismann JS,
552 Jürgens G, Estelle M. 2005. Plant development is regulated by a family of auxin receptor
553 F box proteins. *Dev Cell* **9**:109–119.

554 Eshed Y, Izhaki A, Baum SF, Floyd SK, Bowman JL. 2004. Asymmetric leaf development and
555 blade expansion in Arabidopsis are mediated by KANADI and YABBY activities.
556 *Development* **131**. doi:10.1242/dev.01186

557 Fendrych M, Akhmanova M, Merrin J, Glanc M, Hagihara S, Takahashi K, Uchida N, Torii KU,
558 Friml J. 2018. Rapid and reversible root growth inhibition by TIR1 auxin signalling. *Nat*
559 *Plants* **4**. doi:10.1038/s41477-018-0190-1

560 Finet C, Berne-Dedieu A, Scutt CP, Marlétaz F. 2013. Evolution of the ARF gene family in
561 land plants: Old domains, new tricks. *Mol Biol Evol* **30**:45–56.
562 doi:10.1093/molbev/mss220
563 Finet C, Fourquin C, Vinauger M, Berne-Dedieu A, Chambrier P, Paindavoine S, Scutt CP.
564 2010. Parallel structural evolution of auxin response factors in the angiosperms. *Plant*
565 *Journal* **63**. doi:10.1111/j.1365-313X.2010.04292.x
566 Friml J, Gallei M, Gelová Z, Johnson A, Mazur E, Monzer A, Rodriguez L, Roosjen M,
567 Verstraeten I, Živanović BD, Zou M, Fiedler L, Giannini C, Grones P, Hrtyan M, Kaufmann
568 WA, Kuhn A, Narasimhan M, Randuch M, Rýdza N, Takahashi K, Tan S, Teplova A,
569 Kinoshita T, Weijers D, Rakusová H. 2022. ABP1–TMK auxin perception for global
570 phosphorylation and auxin canalization. *Nature* **609**:575–581. doi:10.1038/s41586-022-
571 05187-x
572 Gietz RD, Schiestl RH. 2007. High-efficiency yeast transformation using the LiAc/SS carrier
573 DNA/PEG method. *Nat Protoc* **2**. doi:10.1038/nprot.2007.13
574 Guilfoyle TJ, Hagen G. 2012. Getting a grasp on domain III/IV responsible for Auxin Response
575 Factor-IAA protein interactions. *Plant Science*. doi:10.1016/j.plantsci.2012.04.003
576 Kato H, Mutte SK, Suzuki H, Crespo I, Das S, Radoeva T, Fontana M, Yoshitake Y, Hainiwa
577 E, van den Berg W, Lindhoud S, Ishizaki K, Hohlbein J, Borst JW, Boer DR, Nishihama
578 R, Kohchi T, Weijers D. 2020. Design principles of a minimal auxin response system. *Nat*
579 *Plants* **6**:473–482. doi:10.1038/s41477-020-0662-y
580 Kelley DR, Arreola A, Gallagher TL, Gasser CS. 2012. ETTIN (ARF3) physically interacts with
581 KANADI proteins to form a functional complex essential for integument development and
582 polarity determination in Arabidopsis. *Development* **139**. doi:10.1242/dev.067918
583 Kepinski S, Leyser O. 2005. The Arabidopsis F-box protein TIR1 is an auxin receptor. *Nature*
584 **435**. doi:10.1038/nature03542
585 Kuhn A, Harborough SR, McLaughlin HM, Natarajan B, Verstraeten I, Friml J, Kepinski S,
586 Østergaard L. 2020. Direct ETTIN-auxin interaction controls chromatin states in
587 gynoecium development. *Elife* **9**. doi:10.7554/eLife.51787
588 Kuhn A, Runciman B, Tasker-Brown W, Østergaard L. 2019. Two auxin response elements
589 fine-tune pinoid expression during gynoecium development in arabidopsis thaliana.
590 *Biomolecules* **9**. doi:10.3390/biom9100526
591 Lavy M, Prigge MJ, Tao S, Shain S, Kuo A, Kirchsteiger K, Estelle M. 2016. Constitutive auxin
592 response in Physcomitrella reveals complex interactions between Aux/IAA and ARF
593 proteins. *Elife*. doi:https://doi.org/10.7554/eLife.13325
594 Liljegren SJ, Roeder AHK, Kempin SA, Gremski K, Østergaard L, Guimil S, Reyes DK,
595 Yanofsky MF. 2004. Control of fruit patterning in Arabidopsis by INDEHISCENT. *Cell* **116**.
596 doi:10.1016/S0092-8674(04)00217-X

597 Lokerse AS, Weijers D. 2009. Auxin enters the matrix - assembly of response machineries for
598 specific outputs. *Curr Opin Plant Biol*. doi:10.1016/j.pbi.2009.07.007
599 Majda M, Robert S. 2018. The role of auxin in cell wall expansion. *Int J Mol Sci*.
600 doi:10.3390/ijms19040951
601 Mi H, Muruganujan A, Ebert D, Huang X, Thomas PD. 2019. PANTHER version 14: More
602 genomes, a new PANTHER GO-slim and improvements in enrichment analysis tools.
603 *Nucleic Acids Res* **47**. doi:10.1093/nar/gky1038
604 Moubayidin L, Østergaard L. 2014. Dynamic control of auxin distribution imposes a bilateral-
605 to-radial symmetry switch during gynoecium development. *Current Biology* **24**.
606 doi:10.1016/j.cub.2014.09.080
607 Nagpal P, Ellis CM, Weber H, Ploense SE, Barkawi LS, Guilfoyle TJ, Hagen G, Alonso JM,
608 Cohen JD, Farmer EE, Ecker JR, Reed JW. 2005. Auxin response factors ARF6 and
609 ARF8 promote jasmonic acid production and flower maturation. *Development* **132**.
610 doi:10.1242/dev.01955
611 Nemhauser JL, Feldman LJ, Zambryski PC. 2000. Auxin and ETTIN in Arabidopsis gynoecium
612 morphogenesis. *Development* **127**. doi:10.1242/dev.127.18.3877
613 Oliveros JC. 2007. VENNY. An interactive tool for comparing lists with Venn Diagrams.
614 http://bioinfogp.cnb.csic.es/tools/venny/index.html.
615 *BioinfogpCnbCsicEs/Tools/Venny/IndexHtml*.
616 Paponov IA, Paponov M, Teale W, Menges M, Chakrabortee S, Murray JAH, Palme K. 2008.
617 Comprehensive transcriptome analysis of auxin responses in Arabidopsis. *Mol Plant*
618 **1**:321–337. doi:10.1093/mp/ssm021
619 Parry G, Calderon-Villalobos LI, Prigge M, Peret B, Dharmasiri S, Itoh H, Lechner E, Gray
620 WM, Bennett M, Estelle M. 2009. Complex regulation of the TIR1/AFB family of auxin
621 receptors.
622 Pekker I, Alvarez JP, Eshed Y. 2005. Auxin response factors mediate Arabidopsis organ
623 asymmetry via modulation of KANADI activity. *Plant Cell* **17**. doi:10.1105/tpc.105.034876
624 Piya S, Shrestha SK, Binder B, Neal Stewart C, Hewezi T. 2014. Protein-protein interaction
625 and gene co-expression maps of ARFs and Aux/IAAs in Arabidopsis. *Front Plant Sci* **5**:1–
626 9. doi:10.3389/fpls.2014.00744
627 Prigge MJ, Platre M, Kadakia N, Zhang Y, Greenham K, Szutu W, Pandey BK, Bhosale RA,
628 Bennett MJ, Busch W, Estelle M. 2020. Genetic analysis of the arabidopsis TIR1/AFB
629 auxin receptors reveals both overlapping and specialized functions. *Elife* **9**.
630 doi:10.7554/eLife.54740
631 Sarojam R, Sappl PG, Goldshmidt A, Efroni I, Floyd SK, Eshed Y, Bowmana JL. 2010.
632 Differentiating Arabidopsis shoots from leaves by combined YABBY activities. *Plant Cell*
633 **22**. doi:10.1105/tpc.110.075853

634 Sessions A, Nemhauser JL, McColl A, Roe JL, Feldmann KA, Zambryski PC. 1997. ETTIN
635 patterns the Arabidopsis floral meristem and reproductive organs. *Development* **124**.
636 doi:10.1242/dev.124.22.4481
637 Siegfried KR, Eshed Y, Baum SF, Otsuga D, Drews GN, Bowman JL. 1999. Members of the
638 YABBY gene family specify abaxial cell fate in Arabidopsis. *Development* **126**.
639 doi:10.1242/dev.126.18.4117
640 Simonini S, Bencivenga S, Trick M, Østergaard L. 2017. Auxin-induced modulation of ETTIN
641 activity orchestrates gene expression in arabidopsis. *Plant Cell* **29**.
642 doi:10.1105/tpc.17.00389
643 Simonini S, Deb J, Moubayidin L, Stephenson P, Valluru M, Freire-Rios A, Sorefan K, Weijers
644 D, Friml J, Østergaard L. 2016. A noncanonical auxin-sensing mechanism is required for
645 organ morphogenesis in Arabidopsis. *Genes Dev* **30**. doi:10.1101/gad.285361.116
646 Szemenyei H, Hannon M, Long JA. 2008. TOPLESS mediates auxin-dependent
647 transcriptional repression during Arabidopsis embryogenesis. *Science (1979)* **319**.
648 doi:10.1126/science.1151461
649 Tiwari SB, Hagen G, Guilfoyle T. 2003. The roles of auxin response factor domains in auxin-
650 responsive transcription. *Plant Cell* **15**:533–543. doi:10.1105/tpc.008417
651 Traas J. 2019. Organogenesis at the shoot apical meristem. *Plants*.
652 doi:10.3390/plants8010006
653 Ulmasov T, Hagen G, Guilfoyle TJ. 1999. Activation and repression of transcription by auxin-
654 response factors. *Proc Natl Acad Sci U S A* **96**. doi:10.1073/pnas.96.10.5844
655 Vernoux T, Brunoud G, Farcot E, Morin V, van den Daele H, Legrand J, Oliva M, Das P,
656 Larrieu A, Wells D, Guédon Y, Armitage L, Picard F, Guyomarc'H S, Cellier C, Parry G,
657 Koumproglou R, Doonan JH, Estelle M, Godin C, Kepinski S, Bennett M, de Veylder L,
658 Traas J. 2011. The auxin signalling network translates dynamic input into robust
659 patterning at the shoot apex. *Mol Syst Biol* **7**. doi:10.1038/msb.2011.39
660 Wang JW, Wang LJ, Mao YB, Cai WJ, Xue HW, Chen XY. 2005. Control of root cap formation
661 by MicroRNA-targeted auxin response factors in Arabidopsis. *Plant Cell* **17**:2204–2216.
662 doi:10.1105/tpc.105.033076
663 Wang W, Xu B, Wang H, Li J, Huang H, Xu L. 2011. YUCCA genes are expressed in response
664 to leaf adaxial-abaxial juxtaposition and are required for leaf margin development. *Plant*
665 *Physiol* **157**. doi:10.1104/pp.111.186395

666

667

668

Figures

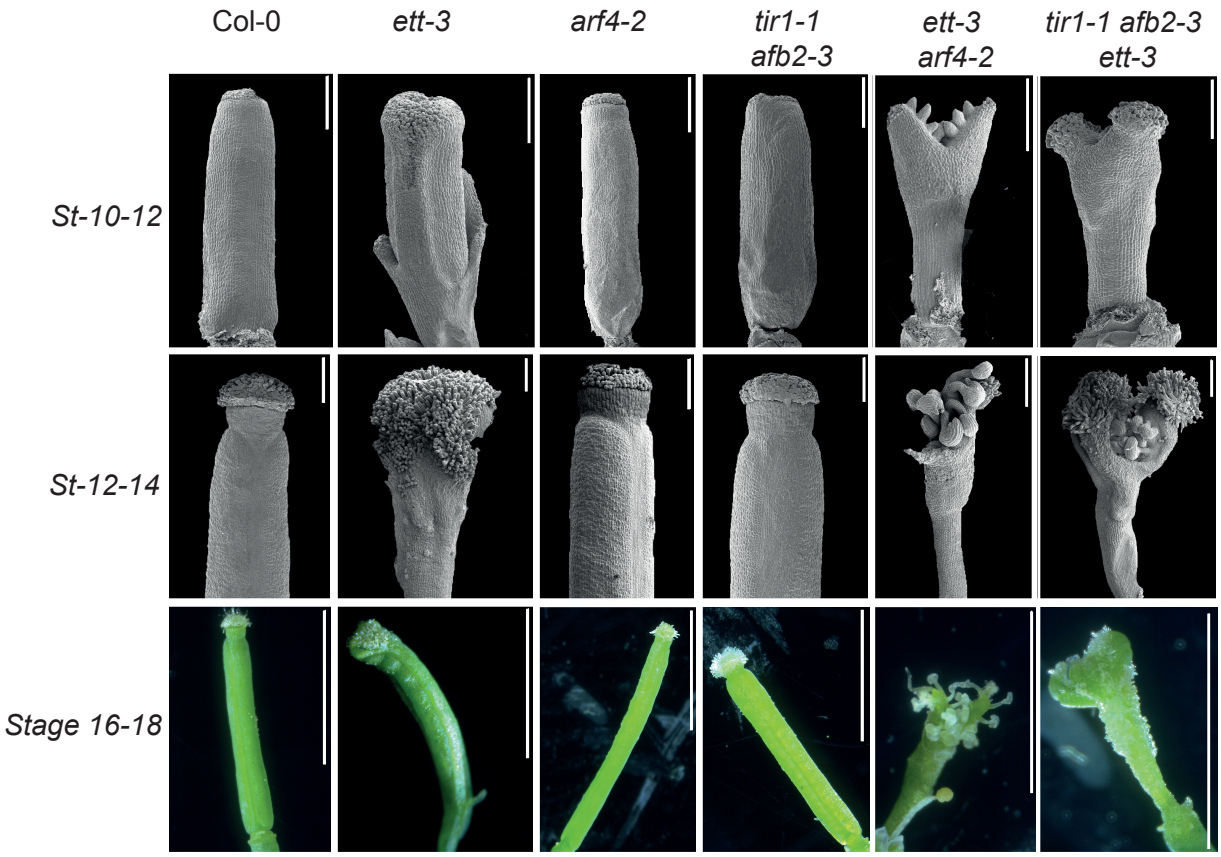

Figure 1: Phenotypes of stage 10-12 and 12-14 gynoecia in scanning electron micrographs (with backgrounds removed for clarity, original images can be seen in Supplemental Figure 1), and photographs of stage 16-18 siliques in Col-0, *ett-3*, *arf4-2*, *tir1-1 afb2-3*, *ett-3 arf4-2* and *tir1-1 afb2-3 ett-3* lines. Scale bars in Scanning electron micrographs show 200 μm in photographs, 3 cm.

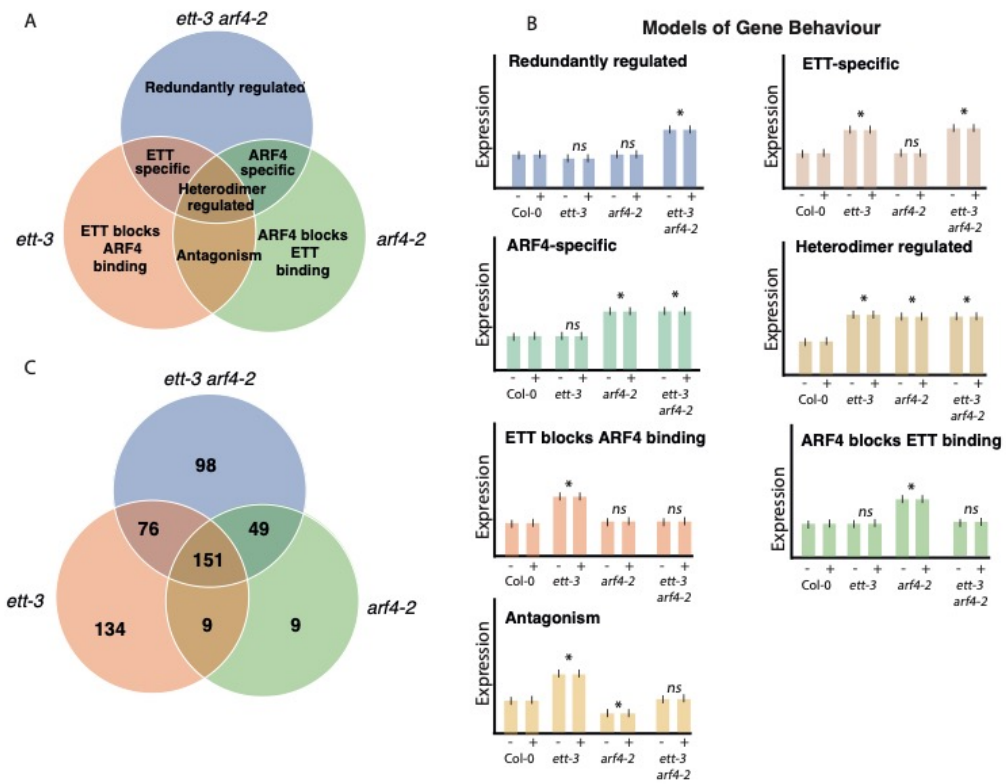

Figure 2: Summary of the findings of the auxin independent analysis A) Venn diagram of the proposed relationships between ETT, ARF4 and downstream targets which are regulated independently of auxin. B) Models of the behaviour of genes which fall into each of these categories, ns, not significant, * significant, -, mock, +, IAA treatment. Whilst the bar charts display an example of genes becoming upregulated in these models, in the datasets analysed they could be up or down regulated. C) Numbers of genes that fall in each sector of the Venn diagram, which are significantly differentially expressed relative to Col-0 in the mutant backgrounds.

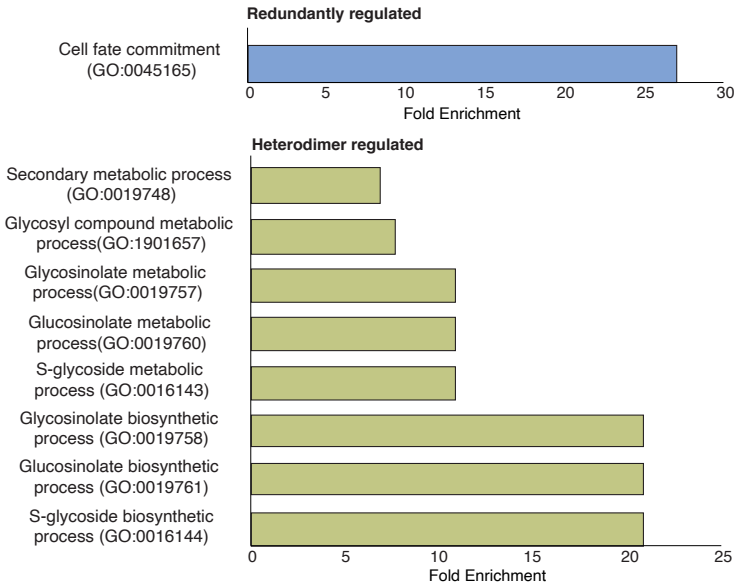

Figure 3: Graphical representation of the significantly enriched GO terms (biological process) identified in PANTHER over/under-representation analysis of the auxin independent dataset.

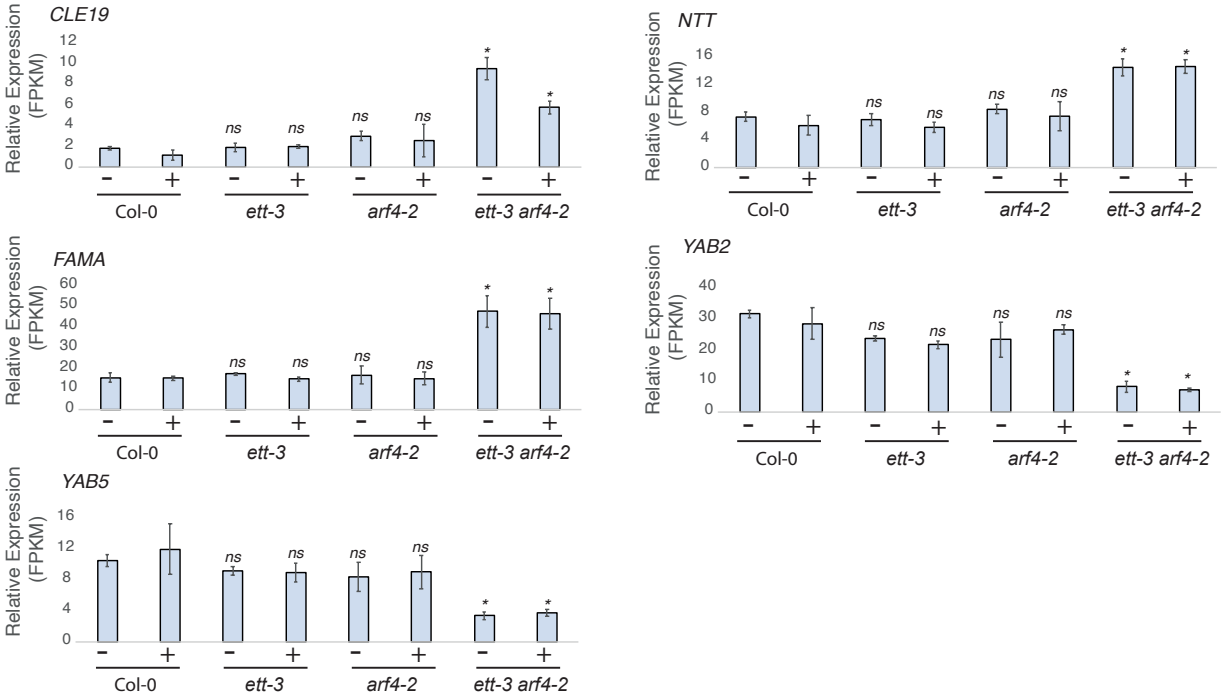

Figure 4: The relative expression (FPKM) of genes involved in cell fate commitment in each genotype after mock (-) or auxin (+) treatment. Statistical analysis was conducted using read count normalization, negative binomial distribution analysis and FDR correction using the BH procedure. The error bars show +/- standard deviation, ns, not significant * = padjust<0.05.

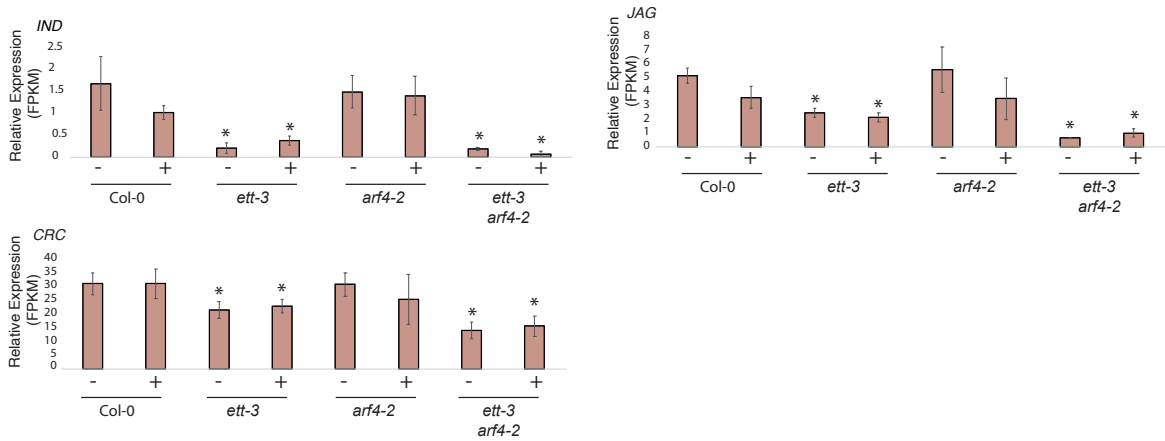

Figure 5: the relative expression (FPKM) of ETT-specific targets with a known role in gynoecium development after mock (-) or auxin (+) treatment. Statistical analysis was conducted using read count normalization, negative binomial distribution analysis and FDR correction using the BH procedure (conducted by Novogene). Error bars show +/- standard deviation, ns, not significant, * = padjust<0.05.

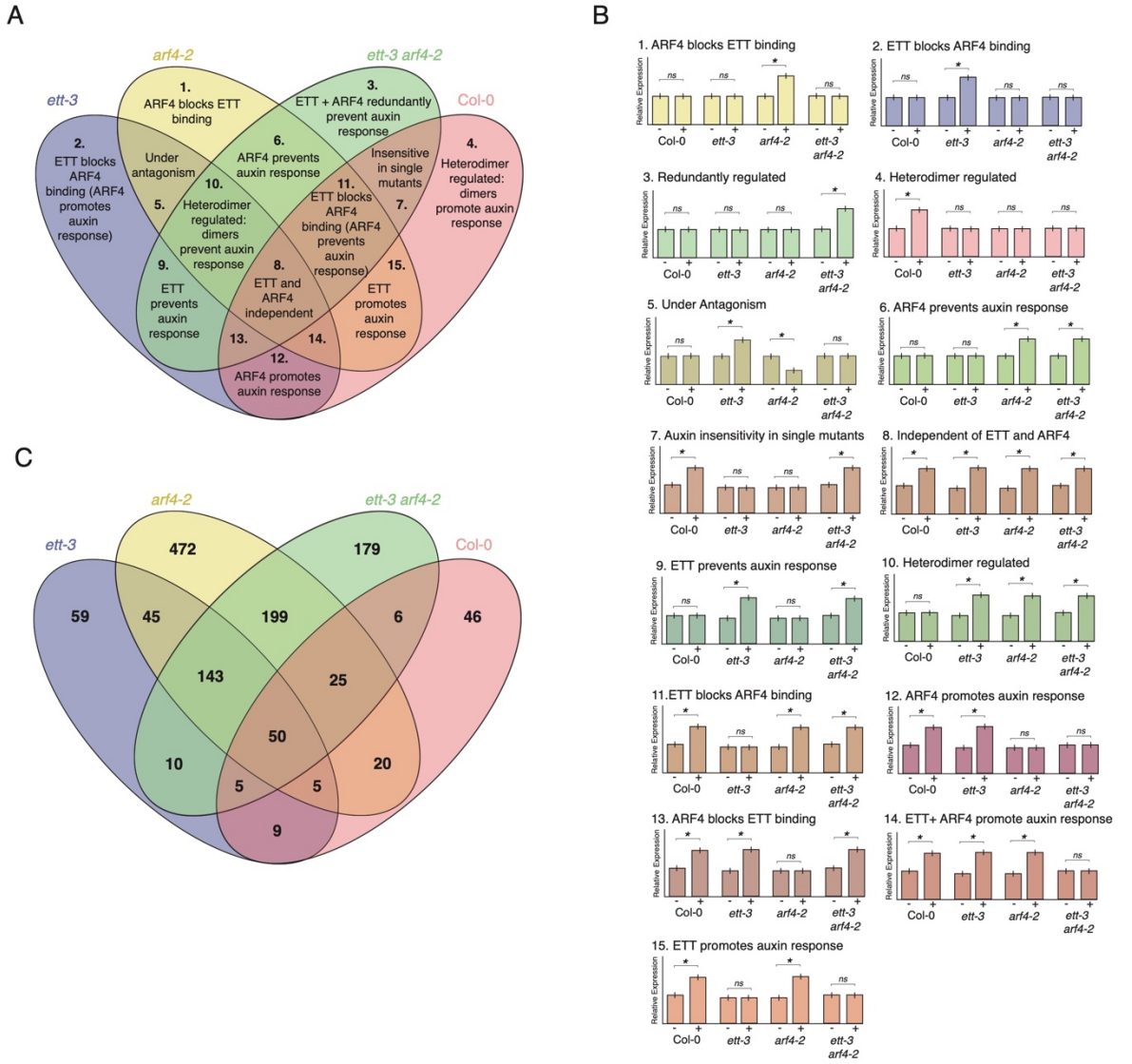

Figure 6: Summary of the findings of the auxin sensitive analysis A) a summary of how the genes in each section of the Venn diagram are predicted to behave, and B) models of gene behaviour corresponding to the segments shown in A after mock (-) or auxin (+) treatment, where * denotes statistical significance. Whilst the examples show genes becoming significantly upregulated in response to auxin in the figure, this is just to demonstrate the patterns of significance expected; in the experimental data the genes could become significantly up or downregulated. C) The number of genes identified which fall into each category of the Venn diagram.

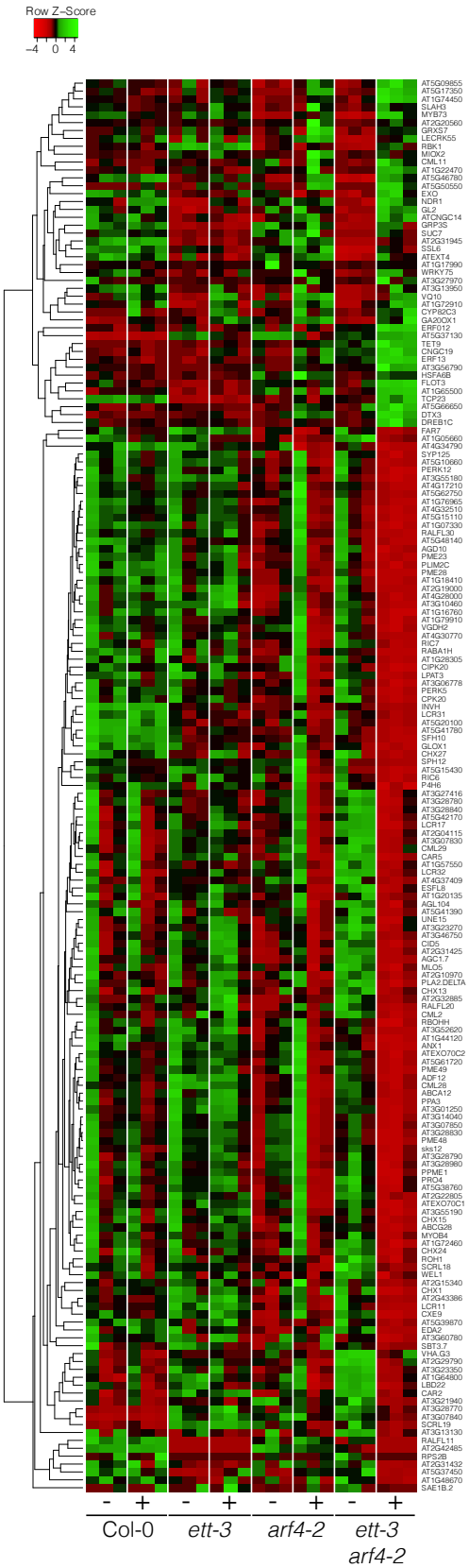

Figure 7: Heatmap showing the genes which become auxin sensitive in the *ett-3 arf4-2* background suggesting that ETT and ARF4 redundantly prevent their auxin responsiveness. Mock and auxin treatment are shown by – and + respectively.

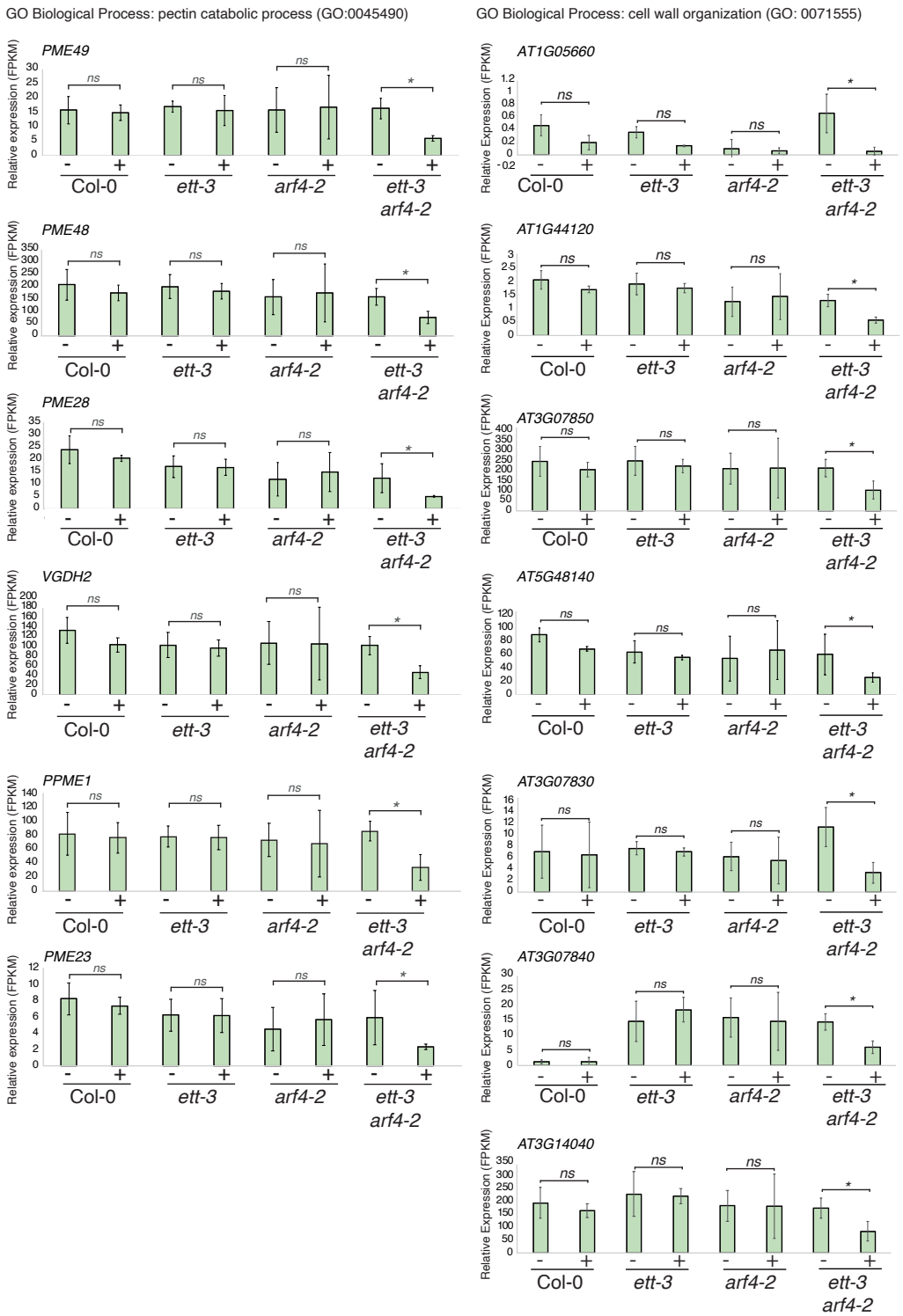

Figure 8: The relative expression (FPKM) of genes involved in pectin catabolism and cell wall organization identified through GO term (biological process) analysis. Statistical analysis was conducted using read count normalization, negative binomial distribution analysis and FDR correction using the BH procedure. The error bars show +/- standard deviation, ns, not significant, * = padjust<0.05. Mock and auxin treatments are shown by – and + respectively.

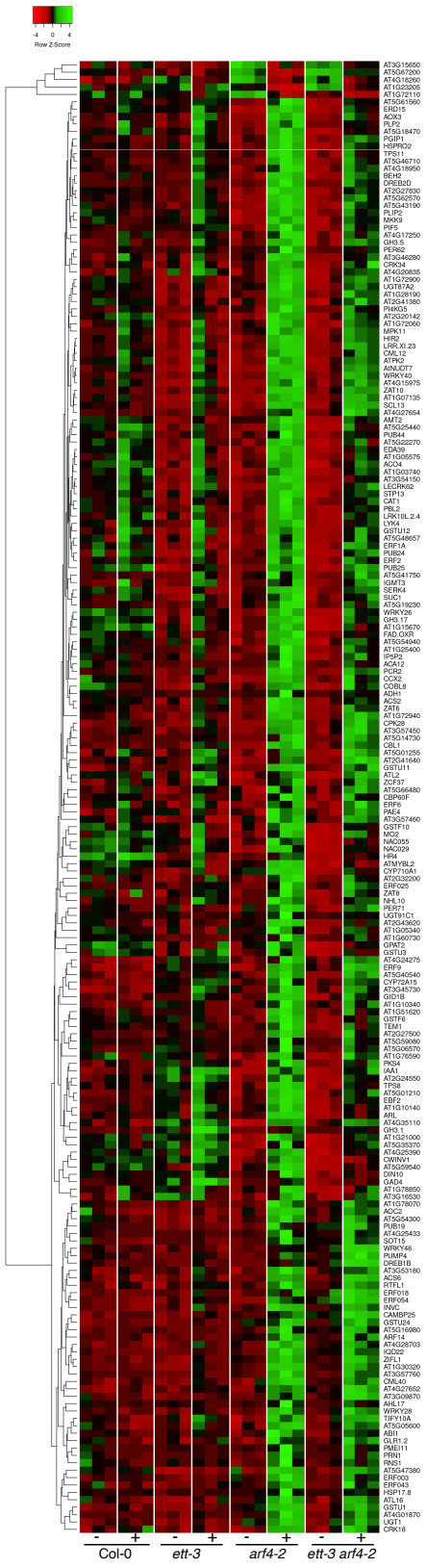

Figure 9**:** Heatmap of genes whose auxin sensitivity is prevented specifically by ARF4. Genes were clustered by average linkage using Spearman's rank correlation. Genes which are highly expressed are shown in green, whilst low expression is shown in red, and mock and auxin treatments are shown by – and + respectively.